

Closed Loop Navigation for Multiple Holonomic Vehicles

Savvas G. Loizou, Kostas J. Kyriakopoulos

Control Systems Laboratory, Mechanical Eng. Dept.
National Technical University of Athens, Greece
{sloizou, kkyria}@central.ntua.gr}

Abstract: *We extend the navigation function methodology, established for single robot navigation, to the case of multiple robots. Appropriate expression of the robot potential functions guarantees global convergence. The derived closed form navigation function provides a robust navigation scheme, suitable for real time implementation. The collision avoidance and global convergence properties are verified through simulations.*

1. Introduction

Navigation of mobile robots has been an area of great research interest in robotics. Most efforts have been focused at the case of a single robot navigating in an environment with obstacles. Recently, navigation for multiple mobile robots is gaining increasing attention. The basic motivation for this work comes from the field of micro robotics, where a team of autonomous micro robots must cooperate to achieve manipulation precision in the sub micron level. Multi robot navigation arises as a basic issue in this task.

There have been several attempts to treat the multi robot navigation problem. Methodologies of motion planning with multiple robots are divided into two large categories. The first category is *Centralized Planning*, which consists of planning the coordinated paths of multiple robots as a path in their composite configuration space: Barraquand, Langlois and Latombe [1] described an **off line** potential field based method to navigate disk shaped robots in narrow corridors. Tournassoud [16] proposed a variant of the potential field approach where motion coordination was expressed as a local optimization problem but global convergence could not be guaranteed since robots could reach a deadlock state where one robot was blocking the other. Barraquand and Latombe ([2,3]) applied randomized path planner – an **off line** potential field based approach that uses random motions to escape local minima. The second category is *Decoupled Planning* ([8,11]), in which paths for each robot are planned independently of other robots and then interactions between paths are considered: O’Donnel and Lozano-Perez [11] proposed *Path Coordination*, a decoupled planning approach based on a scheduling technique for dealing with limited resources. We are mainly interested in on line planners, so we will treat the first category of methodologies.

The multi robot navigation problem we treat in this paper can be stated as follows: “Derive a control law, which drives the robots from any initial configuration to the goal configuration avoiding collisions. The environment is assumed perfectly known and stationary, while each robot has global knowledge of the environment and the team configuration”. Our basic idea is to use the gradient of a potential function to navigate a team of robots, while each robot acts as a potential obstacle to the others.

The rest of the paper is organized as follows: Section 2 outlines the concept of navigation functions. Section 3 introduces the new terminology and the mathematical tools required for the analysis. Section 4 presents simulation results for a number of non-trivial multi robot navigational tasks. Finally, section 5 summarizes the conclusions and indicates our current research.

2. Navigation functions

Navigation functions are real valued maps realized through cost functions, whose negated gradient field is attractive towards the goal configuration and repulsive wrt obstacles. It has been shown by Koditschek and Rimon ([6]) that strict global navigation (i.e. with a globally attracting equilibrium state) is not possible and a smooth vector field on any sphere world, which has a unique attractor, must have at least as many saddles as obstacles. Our assumption that we have spherical robots and spherical obstacles does not constrain the generality of this work since it has been proven that navigation properties are invariant under diffeomorphisms [6]. Methods for constructing analytic diffeomorphisms are discussed in ([12,13]) for point robots and in [14] for rigid body robots.

Let us assume the following situation: We have m mobile robots, and their workspace $W \subset R^2$. Each robot R_i , $i=1\dots m$ occupies a disk in the workspace: $R_i = \{q \in R^2 : \|q - q_i\| \leq r_i\}$ where $q_i \in R^2$ is the center of the disk and r_i is the radius of the robot. The configuration of each robot is represented by q_i and the configuration space C is spanned by $q = [q_1^T \dots q_m^T]^T$.

A navigation function can be defined as follows:

Definition 1: *Let $F \subset R^n$ be a compact connected analytic manifold with boundary. A map $\varphi : F \rightarrow [0,1]$ is a navigation function if: (1) Is analytic on F , (2) It has*

only one minimum at $q_d \in \overset{\circ}{F}$, (3) Its Hessian at all critical points (zero gradient vector field) is full rank and (4) $\lim_{q \rightarrow \partial F} \varphi(q) = 1$

Essentially, the sought control law will be $\dot{q} = u$ where $u = -K \cdot \nabla \varphi(q)$, where K is a gain. We will prove that the class of navigation functions introduced in [6] for single robot navigation, if properly extended, can be used in the multi robot case. We consider the class of navigation functions $\varphi = \sigma_d \circ \sigma \circ \hat{\varphi} = (\gamma/\gamma + G)^{1/k}$ that is a composition of $\sigma_d = x^{1/k}$, $\sigma = x/1+x$ and $\hat{\varphi} = \gamma/G$ the cost function, for which $\gamma^{-1}(0)$ denotes the desirable set and $G^{-1}(0)$ the set, which we want to avoid. A suitable choice is $\gamma = \gamma_d^k$, where $\gamma_d = \|q - q_d\|^2$ is the squared metric of the current configuration q from the destination q_d . The following theorem will help us on deriving results for the function φ by examining the simpler function $\hat{\varphi}$:

Theorem 1 [6]: Let $I_1, I_2 \subseteq \mathbb{R}$ be intervals, $\hat{\varphi}: F \rightarrow I_1$ and $\sigma: I_1 \rightarrow I_2$ be analytic. Define the composition $\varphi: F \rightarrow I_2$, to be $\varphi = \sigma \circ \hat{\varphi}$. If σ is monotonically increasing on I_1 , then the set of critical points of $\hat{\varphi}$ and φ coincide and the (Morse) index of each critical point is identical.

3. Mathematical Tools – Terminology

The robot proximity functions, a measure for the distance between two robots i and j , are defined by: $\beta_{i,j}(q) = q^T D_{ij} q - (r_i + r_j)^2$, where r_i is the radius of the i 'th robot and

$$D_{ij} = \begin{bmatrix} O_{2 \times 2(i-1)} & I_{2 \times 2} & O_{2 \times 2(j-i-1)} & -I_{2 \times 2} & O_{2 \times 2(M-j)} \\ O_{2 \times 2(i-1)} & -I_{2 \times 2} & O_{2 \times 2(j-i-1)} & I_{2 \times 2} & O_{2 \times 2(M-j)} \\ O_{2 \times 2(i-1)} & -I_{2 \times 2} & O_{2 \times 2(j-i-1)} & I_{2 \times 2} & O_{2 \times 2(M-j)} \\ O_{2 \times 2(i-1)} & -I_{2 \times 2} & O_{2 \times 2(j-i-1)} & I_{2 \times 2} & O_{2 \times 2(M-j)} \\ O_{2 \times 2(i-1)} & -I_{2 \times 2} & O_{2 \times 2(j-i-1)} & I_{2 \times 2} & O_{2 \times 2(M-j)} \end{bmatrix}$$

Some useful properties are: $D_{ij} = D_{ij}^T$, $D_{ij} = D_{ji}$, $D_{ij}^k = 2^{k-1} D_{ij}$. We will use the term '**relation**' to describe the possible collision schemes that can be defined in a multi robot - obstacles scene. The **set of relations** between the members of a set can be defined as the set of all possible collision schemes between the members. A **binary relation** is a relation between two robots. Any relation can be expressed as a set of binary relations. A '**relation tree**' is the set of robots-obstacles that form a linked team. Each **relation** may consist of more than one tree (figure 1). We will call the number of binary relations in a relation, the '**relation level**'.

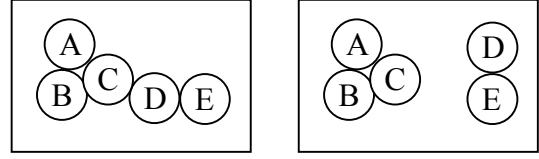


Figure 1: (a) One-tree relation, (b) Two-tree relation

A **relation proximity function (RPF)** provides a measure of the distance between the robots involved in a relation. Each relation has its own RPF. An RPF assumes the value of zero whenever the related robots collide and increases wrt the distance of the related robots:

$$b_{\mathbb{R}} = q^T \cdot P_{\mathbb{R}} \cdot q - \sum_{\{i,j\} \in \mathbb{R}} (r_i + r_j)^2$$

where \mathbb{R} is the set of binary relations (e.g. for the relation in figure 1-b $\mathbb{R} = \{\{A,B\}, \{A,C\}, \{B,C\}, \{D,E\}\}$) and $P_{\mathbb{R}} = \sum_{\{i,j\} \in \mathbb{R}} D_{i,j}$

is the **relation matrix** of RPF.

A **Relation Verification Function (RVF)** is defined by:

$$g_{\mathbb{R}_j} (b_{\mathbb{R}_j}, B_{\mathbb{R}_j^c}) = b_{\mathbb{R}_j} + \lambda \cdot b_{\mathbb{R}_j^c} / (b_{\mathbb{R}_j} + B_{\mathbb{R}_j^c}^{h/\lambda}) \quad (3.1)$$

where $\lambda, h > 0$, \mathbb{R}_j^c is the complementary to \mathbb{R}_j set of relations in the same level, j is an index number defining the relation in the level and $B_{\mathbb{R}_j^c} = \prod_{k \in \mathbb{R}_j^c} b_k$. An

RVF is zero if a relation holds while no other relation from the same level holds and has the properties:

$$(a) \lim_{x \rightarrow 0} \lim_{y \rightarrow 0} g_x(x, y) = \lambda, (b) \lim_{y \rightarrow 0} \lim_{x \rightarrow 0} g_x(x, y) = 0.$$

Based on the above properties, in a robot proximity situation, one can verify that: if $(g_{\mathbb{R}_j})_k = 0$ at some level k then $(g_{\mathbb{R}_h})_k \neq 0$ for any level h and $i \neq j$ in level k .

We can now define $G = \prod_{L=1}^{n_L} \prod_{j=1}^{n_{R,L}} (g_{\mathbb{R}_j})_L$, with n_L the number of levels and $n_{R,L}$ the number of relations in level L . Figure 2 demonstrates several types of relations of a four-member team.

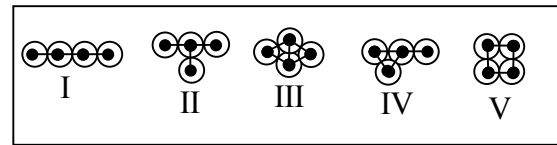


Figure 2: I, II are level 3; IV, V are level 4 and III is a level 5 relation

3.1. Proof of correctness

Let $\varepsilon > 0$. Define $B_i^l(\varepsilon) = \{q : 0 < (g_{\mathbb{R}_i}(q))_l < \varepsilon\}$. We can then discriminate the following topologies:

1. The destination point q_d
2. The free space boundary: $\partial F(q) = G^{-1}(\delta)$, $\delta \rightarrow 0$

3. The robot/obstacle proximity set:

$$F_0(\varepsilon) = \bigcup_{L=1}^{n_L} \bigcup_{i=1}^{n_{R,L}} B_i^L(\varepsilon) - \{q_d\}, \text{ with } n_L \text{ and } n_{R,L} \text{ as defined}$$

above.

4. The robot/obstacle distant set:

$$F_1(\varepsilon) = F - (\{q_d\} \cup F_0(\varepsilon))$$

Proposition 1: The destination point q_d is a non-degenerate local minimum of φ .

Proof: Similar¹ to this found in [6].

Proposition 2: All the critical points are in the interior of the free space

Proof: Let q_0 be a point on ∂F and suppose that

$$(\mathbf{g}_{R_j})_{\kappa}(q_0) = 0 \text{ for the relation } j \text{ of level } k. \text{ Then}$$

$$(\mathbf{g}_{R_h})_h(q_0) > 0, \text{ for any level } h \text{ and } i \neq j \text{ in level } k,$$

because only one RVF can hold at a time. Then at q_0 :

$$\nabla \varphi(q_0) = \left((\gamma_d^k + G)^{1/k} \nabla \gamma_d - \gamma_d \nabla (\gamma_d^k + G)^{1/k} \right) \dots$$

$$\dots / (\gamma_d^k + G)^{2/k} = -\frac{1}{k} \gamma_d^{-k} \left(\prod_{L=1}^{n_L} \prod_{\substack{i=1 \\ i \neq j}}^{n_{R,L}} (\mathbf{g}_{R_i})_L \right) \nabla (\mathbf{g}_{R_j})_{\kappa} \neq 0$$

Proposition 3: For every $\varepsilon > 0$, there exists a positive integer $N(\varepsilon)$ such that if $k > N(\varepsilon)$ then there are no critical points of $\hat{\varphi}$ in $F_1(\varepsilon)$.

Proof: Similar to this found in [6].

Proposition 4: There exists an $\varepsilon_0 > 0$, such that $\hat{\varphi}$ has no local minimum in $F_0(\varepsilon)$, as long as $\varepsilon < \varepsilon_0$.

Proof: If $q \in F_0(\varepsilon) \cap C_{\hat{\varphi}}$, where $C_{\hat{\varphi}}$ is the set of critical points, then $q \in B_i^L(\varepsilon)$ for at least one set $\{L, i\}$,

$i \in \{1..n_{R,L}\}$, $L \in \{1..n_L\}$ with n_L the number of levels

and $n_{R,L}$ the number of relations in level L . We will use

a unit vector as a test direction to demonstrate that $(\nabla^2 \hat{\varphi})(q)$ has at least one negative eigenvalue. At a

critical point, $(\nabla \hat{\varphi})(q) = 0$ and the Hessian:

$$(\nabla^2 \hat{\varphi})(q) =$$

$$\gamma_d^{k-1} \left(kG \cdot \nabla^2 \gamma_d + (1-1/k) \frac{\gamma_d}{G} \nabla G \cdot \nabla G^T - \gamma_d \cdot \nabla^2 G \right) / G^2$$

We choose the test vector to be: $\hat{u} = P_R \cdot q^\perp / \|P_R \cdot q^\perp\|$

where P_R is the relation matrix of b_R and

$q^\perp = [q_1^\perp \dots q_m^\perp]$. With $\nabla^2 \gamma_d = 2I$ we form the quadratic form:

$$(G^2 / \gamma_d^{k-1}) \hat{u}^T (\nabla^2 \hat{\varphi})(q) \hat{u} = 2kG + \dots \quad (3.2)$$

$$\dots + (1-1/k) (\gamma_d / G) \hat{u}^T \cdot \nabla G \cdot \nabla G^T \cdot \hat{u} - \gamma_d \cdot \hat{u}^T \cdot \nabla^2 G \cdot \hat{u}$$

With proper manipulation, one can verify that $\hat{u} \perp \nabla b_R$

and $\hat{u}^T \cdot \nabla^2 \mathbf{g}_{R_i} \cdot \hat{u} = v_i \cdot c_i + b_i \cdot \hat{u}^T A_i \hat{u}$ where $v_i \geq 2$,

$\tilde{b}_i \equiv B_{R_i^c}$, $c_i = (1 + \lambda / (b_{R_i} + \tilde{b}_i^{1/h}))$ and A_i can be found in

Appendix. If $\mu_i = \nabla b_R \cdot \nabla \gamma_d / 2 - v_i \cdot \gamma_d$, after

manipulation (3.2) becomes:

$$\frac{G^2}{\gamma_d^{k-1}} \hat{u}^T (\nabla^2 \hat{\varphi})(q) \hat{u} = \bar{g}_i c_i \mu_i + \mathbf{g}_{R_i} (\gamma_d \eta_i - \gamma_d \xi_i - \sigma_i + \nabla \bar{g}_i \nabla \gamma_d)$$

where $G = \mathbf{g}_{R_i} \cdot \bar{g}_i$, and η_i , ξ_i and σ_i are in Appendix.

The second term is proportional to \mathbf{g}_{R_i} and can be made arbitrarily small by a choice of ε but can still be positive, so the first term should be strictly negative.

Lemma 1:

$$\max_{q \in F_0} (\mu_i) = (x+a) \cdot (x-a/(m-1)) \cdot (m-1)/m$$

$$\text{where } x = \sqrt{\varepsilon + \sum (r_i + r_j)^2}, \quad a = \sqrt{q_d^T P_R q_d}$$

Proof: $\mu_i = \nabla b_R \cdot \nabla \gamma_d / 2 - v_i \cdot \gamma_d \leq 2f(q)$ where

$f(q) = q^T \cdot P_R \cdot q - q^T \cdot P_R \cdot q_d - (q - q_d)^T \cdot (q - q_d)$. Thus

$\nabla f(q) = 2P_R \cdot q - P_R \cdot q_d - 2(q - q_d)$. At a critical point

q_c , it will be: $\nabla f(q_c) = 0$. Solving for q_c , we get:

$q_c = 1/2 \cdot (P_R - I)^{-1} \cdot (P_R - 2I) \cdot q_d$. But for the worst-

case scenario $(P_R - I)^{-1} = 1/(m-1) \cdot P_R - I$ with

$$P_R = m \cdot I - [1 \dots 1]^T [1 \dots 1]. \quad \text{So}$$

$$q_c = (I - P_R \cdot 1/(2m-2)) q_d \quad \text{and}$$

$f(q_c) = -m/(4m-4) < 0$. The Hessian of $f(q)$ is:

$$\nabla^2 f(q) = 2(P_R - I). \text{ It can be verified that } P_R - I \text{ has}$$

eigenvalues: (i) $\lambda = m-1$ of multiplicity $(m-1)D$,

where D is the workspace dimension, and (ii) $\lambda = -1$ of multiplicity D . That means that $f(q)$ decreases only

along D dimensions about q_c and increases along the

$(m-1)D$ remaining (for some appropriate coordinate

system), which in turn means that q_c is a saddle. We are

interested in finding the maximum value that $f(q)$ may

attain under the constraint that $b_R \leq \varepsilon$. We form the

constraint function:

¹ Due to space limits a number of proofs will be omitted but can be sent upon request to the Conference IPC.

$g(q) = q^T \cdot P_R \cdot q - \varepsilon - \sum_{\{i,j\} \in \mathbb{R}} (r_i + r_j)^2 \leq 0$. Since g is convex ($\nabla^2 g(q) = 2 \cdot P_R > 0$) and q_c is a saddle point of f , $f(q)$ will attain its maximum and minimum values over the constraint's boundary, $g(q) = 0$. This can be formulated as a nonlinear optimization problem:

$$\max_{q \in U} (f(q))$$

where

$$f(q) = q^T \cdot P_R \cdot q - q^T \cdot P_R \cdot q_d - (q - q_d)^T \cdot (q - q_d)$$

and

$$U = \left\{ q : g(q) = q^T \cdot P_R \cdot q - \varepsilon - \sum_{\{i,j\} \in \mathbb{R}} (r_i + r_j)^2 \leq 0 \right\}$$

If $q^* = \arg \max_{q \in U} (f(q))$ then, according to Kuhn Tucker conditions, there exists a $\rho \geq 0$ such that:

$$\nabla f(q^*) - \rho \nabla g(q^*) = 0 \quad (3.3) \text{ (a)}$$

$$\rho \cdot g(q^*) = 0 \quad (3.3) \text{ (b)}$$

$$g(q^*) \leq 0 \quad (3.3) \text{ (c)}$$

$$\rho \geq 0 \quad (3.3) \text{ (d)}$$

From (3.3) (a) we have:

$$2P_R \cdot q^* - P_R \cdot q_d - 2(q^* - q_d) - 2\rho \cdot P_R \cdot q^* = 0. \text{ Solving}$$

for q^* , $q^* = (1/2)(I + (\rho - 1) \cdot P_R)^{-1} (2I - P_R) q_d$. One can easily verify that

$$(I + (\rho - 1) \cdot P_R)^{-1} = (I - P_R \cdot (\rho - 1)) / (1 + (\rho - 1)m)$$

and $q^* = 1/2 \cdot (2I - P_R \cdot (2\rho - 1)) / (1 + (\rho - 1)m) q_d$. As

discussed above, the constraint should be activated, so $\rho > 0$ and from (3.3)(b) we get: $g(q^*) = 0$. Solving for

$$\rho : \rho_{1,2} = (2(m-1) \pm (m-2)a/x) / (2m). \text{ Both } \rho_1, \rho_2$$

could be made positive so by substituting in q^* :

$${}^+q^* = (I - P_R(a+x)) / (ma) q_d,$$

$${}^-q^* = (I - P_R(a-x)) / (ma) q_d,$$

where ${}^+q^*$, ${}^-q^*$ are the values of q^* for ρ_1, ρ_2 respectively. Examining the terms of $f(q)$, we have:

$$(i) q^T P_R q = x^2 \text{ for both } {}^+q^*, {}^-q^*,$$

$$(ii) q^T P_R q_d = -ax \text{ for } {}^+q^*,$$

$$(iii) q^T P_R q_d = ax \text{ for } {}^-q^*,$$

$$(iv) (q - q_d)^T (q - q_d) = (a+x)^2 / m \text{ for } {}^+q^* \text{ and}$$

$$(v) (q - q_d)^T (q - q_d) = (a-x)^2 / m \text{ for } {}^-q^*.$$

After substituting in $f(q)$, we get:

$$f({}^+q^*) = x^2 + ax - (a+x)^2 / m = \dots$$

$$\dots = (x+a)(x-a/(m-1))(m-1)/m$$

$$\text{and } f({}^-q^*) = x^2 - ax - (a-x)^2 / m = \dots$$

$$\dots = (x+a/(m-1))(x-a)(m-1)/m$$

Then $f({}^+q^*) < 0$ for $-a < x < a/(m-1)$ and

$f({}^-q^*) < 0$ for $-a/(m-1) < x < a$. We can observe that

$f({}^+q^*) = f({}^-q^*)$ for $x = 0$ and since we are interested

for $x > 0$, it holds that $f({}^+q^*) > f({}^-q^*)$ since

$$f({}^+q^*) - f({}^-q^*) = 2 \cdot a \cdot m \cdot x / (1+m) > 0, \forall x > 0.$$

Therefore, by choosing $f({}^+q^*)$ we have the result:

$$\max_{q \in F_0} (\mu_i) = (x+a) \cdot (x-a/(m-1)) \cdot (m-1) / m \text{ and the}$$

proof of Lemma 1 is complete. \square

So according to Lemma 1, for μ_i to be negative, it is sufficient to make sure that:

$$\varepsilon < q_d^T P_R q_d / (m-1)^2 - \sum_{\{i,j\} \in \mathbb{R}} (r_i + r_j)^2 = \dots$$

$$\dots = \sum_{\{i,j\} \in \mathbb{R}} \|q_d^i - q_d^j\|^2 / (m-1)^2 - \sum_{\{i,j\} \in \mathbb{R}} (r_i + r_j)^2 = \varepsilon_0$$

Another constraint arises from the fact that $\varepsilon > 0$. So for a valid workspace it will be:

$$\sum_{\{i,j\} \in \mathbb{R}} \|q_d^i - q_d^j\|^2 > (m-1)^2 \cdot \sum_{\{i,j\} \in \mathbb{R}} (r_i + r_j)^2 \text{ for every } \mathbb{R}_j.$$

This condition establishes that goal configurations are achievable (not any collisions at the target) and that there will always be a direction of movement decreasing the potential function. \blacksquare

4. Simulation results

To verify the navigation properties of the function we derived, we set up a simulation with three and four holonomic robots that are about to navigate from an initial to a final configuration, without hitting each other. The robots are placed at several initial configurations and the paths traveled are recorded and depicted in the figures that follow. The chosen configurations constitute non-trivial setups since the straight paths connecting initial and final positions of each robot are obstructed by other robots.

In the first case (Fig (3a)), three robots were positioned at

$$\begin{bmatrix} q_1^T & q_2^T & q_3^T \end{bmatrix}^T = [0 \ 0.070 \ 0.061 \ -0.035 \ -0.061 \ -0.035],$$

and their destination configuration was set at:

$$\begin{bmatrix} {}^d q_1^T & {}^d q_2^T & {}^d q_3^T \end{bmatrix}^T = [0 \ -0.2 \ -0.1732 \ 0.1 \ 0.1732 \ 0.1]$$

Figures (3b,c) depict the trajectories of the robots. As it

can be seen, the navigation function performs very well in this case.

In the second case (Fig 4a), three robots were positioned at $[q_1^T \ q_2^T \ q_3^T]^T = [-0.2 \ 0.1 \ 0.0 \ 0.1 \ 0.2 \ 0.1]$, and their destination configuration was set at: $[{}^d q_1^T \ {}^d q_2^T \ {}^d q_3^T]^T = [0.2 \ 0.0 \ -0.2 \ 0.0 \ 0.0 \ 0.0]$ Figures (4b), (4c) and (4d) depict the trajectories of the robots. As can be seen the navigation function successfully resolves all the proximity situations.

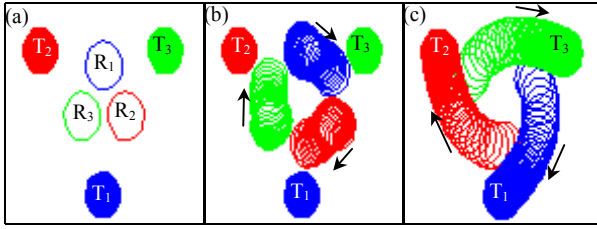


Figure 3: (a) Initial Conf., (b) Intermediate Conf., (c) Intermediate and Final Configurations.

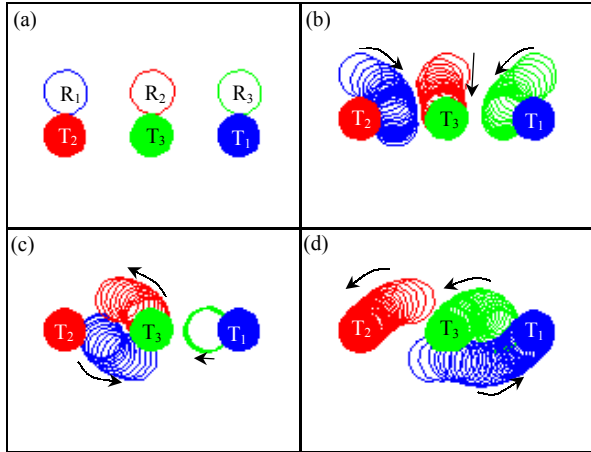


Figure 4: (a) Initial Conf., (b), (c) Intermediate Conf., (d) Intermediate and Final Configurations.

In the next set of simulations, we had four robots. To demonstrate the robustness of the method we set up two scenarios: In the first (fig. 5), a robot (R₄) was placed at its goal position and the other three were about to navigate from an initial position to their goal. Their initial configuration was set at: $[q_1^T \ q_2^T \ q_3^T \ q_4^T]^T = [0.173 \ -0.1 \ -0.173 \ -0.1 \ 0.0 \ 0.2 \ 0.0 \ 0.0]$ and their destination was set $[{}^d q_1^T \ {}^d q_2^T \ {}^d q_3^T \ {}^d q_4^T]^T = [-0.173 \ 0.1 \ 0.173 \ 0.1 \ 0.0 \ -0.2 \ 0.0 \ 0.0]$. Figure 5 depicts the trajectories of the robots. Notice there that the robot R₄ is temporarily relocated to assist the motion of the rest robots.

In the second case (fig. 6), robot R₄ was “immobilized” to represent an obstacle O₁. Thus, the initial and final configurations were set to be:

$[q_1^T \ q_2^T \ q_3^T]^T = [0.173 \ -0.1 \ -0.173 \ -0.1 \ 0.0 \ 0.2]$ and $[{}^d q_1^T \ {}^d q_2^T \ {}^d q_3^T]^T = [-0.173 \ 0.1 \ 0.173 \ 0.1 \ 0.0 \ -0.2]$. Our methodology succeeded in finding a collision free set of trajectories, in this case too.

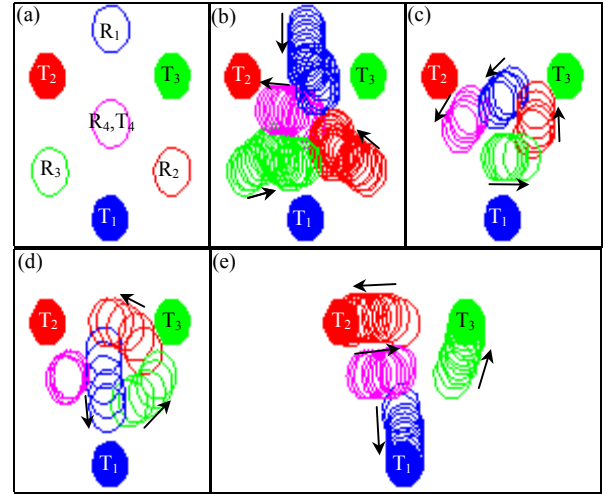


Figure 5: (a) Initial Conf., (b), (c), (d) Intermediate Conf., (e) Intermediate and Final Configurations.

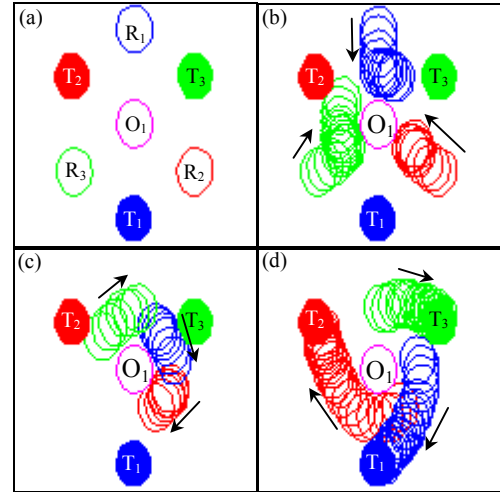


Figure 6: (a) Initial Conf., (b), (c) Intermediate Conf., (d) Intermediate and Final Configurations.

5. Conclusions – Issues for Further Research

In this paper, a methodology for multiple holonomic mobile robot navigation is presented. The methodology extends the single robot navigation methodology established by [6] to the multiple robot case and is designed to account for the volume of the robots. The robot – obstacle potentials used in the single robot

navigation, are now replaced by appropriately constructed robot proximity potentials (*RVPs*), which capture all the possible multi robot proximity situations. The methodology due to its closed loop nature provides a robust navigation scheme with guaranteed collision avoidance and it's global convergence properties guarantee that a solution will be found if one exists. Analytic expressions of the potential function and its derivatives make the methodology particularly suitable for real time implementation. The method can be applied to a three dimensional workspace and through proper transformations to robots arbitrarily shaped. The effectiveness of the methodology is verified through computer simulations. The complexity of the method increases rapidly wrt number m of robots since the

number M of *RVPs* will be $M = 2^{\binom{m}{2}} - 1$ which for e.g. 5 robots is $M = 1023$.

Current research directions are towards decentralized multiple robot navigation with limited workspace knowledge, limited vision capability, cooperation between mobile robots, consideration of non-holonomic and under-actuated mobile robots as well as locomotion issues in the context of micro robotics.

Acknowledgements: The authors want to acknowledge the contribution of the European Commission through contract IST-2001-33567 - MICRON

References

- [1] J. Barraquand, B. Langlois and J.C. Latombe, "Numerical Potential Field Techniques For Robot Path Planning," IEEE Trans. on Systems, Man and Cybernetics, vol. 22 (2) pp.: 224-241, 1992.
- [2] J. Barraquand, J.C. Latombe, "A Monte Carlo algorithm for path planning with many degrees of freedom," Proc. of IEEE Int. Conf. on Robotics and Automation, pp.:1712-1717, 1990
- [3] J. Barraquand, J.C. Latombe, "A distributed representation Approach," Int. Journal of Robotics Research, 10(6),pp.:628-649, 1991
- [4] D. Bertsekas, "Nonlinear Programming," Athena Scientific, 1995.
- [5] D. E. Koditschek, "Robot Planning and Control via Potential Functions," The Robotics Review, MIT Press, pp.:349-368, 1989.
- [6] D.E. Koditschek and E. Rimon, "Robot navigation functions on manifolds with boundary," Advances Appl. Math., vol. 11, pp. 412-442, 1990
- [7] J.C. Latombe, "Robot Motion Planning," Kluwer Academic Publishers, 1991.
- [8] Y.H. Liu, S. Kuroda, T. Naniwa, H. Noborio and S. Arimoto, "A practical algorithm for planning collision free coordinated motion of multiple mobile robots," in Proc of IEEE Int. Conf. on Robotics and Automation, pp.:1427-1432, 1989..
- [9] V. J. Lumelsky and K. R. Harinarayan, "Decentralized motion planning for multiple mobile robots: The cocktail

party model," Journal of Autonomous Robots, (4): 121-135, 1997.

- [10] J. Milnor, "Morse theory," Annals of Mathematics Studies, Princeton University Press, Princeton, NJ, 1963.
- [11] P.A. O'Donnel and T. Lozano-Pérez, "Deadlock-free and collision-free coordination of two robotic manipulators," In Proc. of IEEE int. Conf. on Robotics and Automation, pp.: 484-489, 1989.
- [12] E. Rimon and D. E. Koditschek, "Exact Robot Navigation Using Artificial Potential Functions," IEEE Trans. on Robotics and Automation, vol. 8, No. 5, pp. 501-518, 1992
- [13] E. Rimon and D. E. Koditschek, "The Construction of Analytic Diffeomorphisms for Exact Robot Navigation on Star Worlds," Trans. of the American Mathematical Society, vol. 327, no. 1, pp. 71-115, Sept. 1991.
- [14] H. G. Tanner, S. G. Loizou and K. J. Kyriakopoulos, "Nonholonomic Stabilization with Collision Avoidance for Mobile Robots," Proc. of the 2001 IEEE/RSJ Int. Conf. on Intelligent Robots and Systems, pp. 1220-1225
- [15] E. Todt, G. Raush and R. Suarez, "Analysis and Classification of Multiple Robot Coordination Methods," Proc. of the 2000 IEEE Int. Conf. on Robotics and Automation, pp. 3158-3163.
- [16] P. Tournassoud, "A Strategy For Obstacle Avoidance And Its Applications To Multi - Robot Systems," Proc. of IEEE Int. Conf. on Robotics and Automation, pp. 1224-1229, 1986

APPENDIX

$$\begin{aligned}
 A_i &= \lambda \left[2 \frac{(\nabla b_R + \nabla \tilde{b}_i^{1/h})(\nabla b_R + \nabla \tilde{b}_i^{1/h})^T}{(b_R + \tilde{b}_i^{1/h})^3} - \frac{(\nabla^2 b_R + \nabla^2 \tilde{b}_i^{1/h})}{(b_R + \tilde{b}_i^{1/h})^2} \right] \\
 \eta_i &= \left(\frac{\hat{u}^T \cdot \nabla \bar{g}_i \cdot \nabla \bar{g}_i^T \cdot \hat{u}}{\bar{g}_i} + \frac{\lambda^2 \cdot \bar{g}_i \cdot \hat{u}^T \cdot \nabla(\tilde{b}_i^{1/h}) \cdot \nabla(\tilde{b}_i^{1/h})^T}{c_i^2 (b_R + \tilde{b}_i^{1/h})^4} \dots \right. \\
 &\quad \left. \dots - \frac{2\lambda}{c_i \cdot (b_R + \tilde{b}_i^{1/h})^2} \hat{u}^T \cdot \nabla(\tilde{b}_i^{1/h}) \cdot \nabla \bar{g}_i^T \cdot \hat{u} \right) \left(1 - \frac{1}{k} \right) \\
 \xi_i &= \hat{u}^T \cdot \nabla^2 \bar{g}_i \cdot \hat{u} + \frac{\bar{g}_i}{c_i} \cdot \hat{u}^T \cdot A_i \cdot \hat{u} \dots \\
 &\quad \dots - 2 \frac{\lambda}{c_i (b_R + \tilde{b}_i^{1/h})^2} \hat{u}^T \cdot \nabla(\tilde{b}_i^{1/h}) \cdot \nabla \bar{g}_i \cdot \hat{u} \\
 \sigma_i &= \frac{\lambda \bar{g}_i}{2c_i (b_R + \tilde{b}_i^{1/h})^2} (\nabla b_R + \nabla \tilde{b}_i^{1/h}) \cdot \nabla \gamma_d
 \end{aligned}$$